AD-A113 752 NORTHWESTERN UNIV EVANSTON IL DEPT OF MATERIALS SCIENCE F/G 20/3
EFFECT OF GRADIENTS IN MULTI-AXIAL STRESS STATES ON RESIDUAL ST--ETC(U)
MAR 82 I C NOYAN N00014-80-C-0116
UNCLASSIFIED TR-6 NL

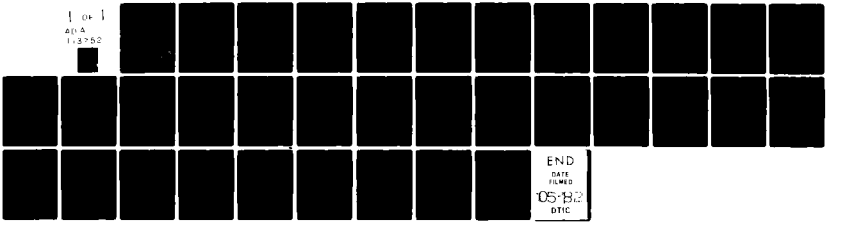

NORTHWESTERN UNIVERSITY

DEPARTMENT OF MATERIALS SCIENCE

Technical Report No. 6
March 30, 1982

Office of Navil Research
Contract N00014-80-C-0116

EFFECT OF GRADIENTS IN MULTI-AXIAL STRESS STATES ON RESIDUAL STRESS MEASUREMENTS WITH X-RAYS

by

I. C. Noyan

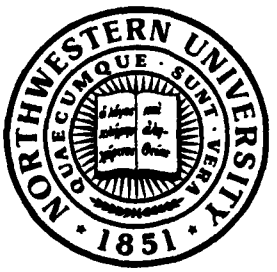

EVANSTON, ILLINOIS

EFFECT OF GRADIENTS IN MULTI-AXIAL STRESS STATES ON RESIDUAL STRESS MEASUREMENTS WITH X-RAYS

by

I. C. Noyan*

ABSTRACT

The assumption, that stress components in the direction of the surface normal are negligible in traditional residual stress determination methods by x-rays, has been recently disproved. In this paper we investigate the effect of normal stresses on the accuracy of these traditional methods. It is shown that appreciable error can exist in surface stresses determined by such methods, if normal stresses are present. New procedures are proposed to minimize these errors.

*Graduate student and Research Assistant, Dept. of Materials Science and Engineering, The Technological Institute, Northwestern University, Evanston Illinois 60201

INTRODUCTION

The determination of surface residual stresses in poly-crystalline materials by X-ray methods is well established.[1,2] Traditional methods assume a bi-axial stress state that is uniform in the surface layers penetrated by the x-ray beam. This assumption is based on the conception that this penetration depth is too low to be affected by the stresses in the third dimension. These methods predict a linear variation of inter-planar spacing "d" with "$\sin^2\psi$", with a slope that is proportional to the stress in the measurement direction ($\underline{S}_\phi$); here ψ is the angle between the normal to the diffracting planes ($\underline{L}_3$) and the surface normal of the specimen ($\underline{S}_3$), as shown in figure 1. If the components of the (assumed) bi-axial stress tensor exhibit steep gradients in the volume sampled by the x-ray beam, curvature occurs in the "d" vs $\sin^2\psi$ plot. The slope of a least-square fit to such data yields the stress in the ($\underline{S}_\phi$) direction, averaged over the depth of penetration.[3]

The assumption in these traditional methods, that stress components in the direction of the surface normal ($\underline{S}_3$) are negligible in the volume sampled by the x-ray beam has been disproved in several recent studies.[4,5] Stress components of appreciable magnitude in this direction have been detected in the surface layers of materials, created in various ways. Recent theory, as well as experiments, show that if stresses (σ_{13},σ_{23}) in the direction of the surface normal ($\underline{S}_3$) are present, "splitting" of the "d" vs $\sin^2\psi$ data results; that is "d" vs $\sin^2\psi$ plots have opposite curvature for negative and positive ψ. Analysis of such data is described in detail by Dölle,[6] (see also reference 4 for an example of the use of this analysis). If, however, only normal stress (σ_{33}) is present in the direction of the surface normal and shear components are negligible, curvature occurs in the "d" vs $\sin^2\psi$ data and there is no "ψ-splitting". The degree of such curvature depends on the steepness of the gradient in σ_{33}. (Since σ_{33} is a stress normal to the surface, it is zero, by definition at the surface. Thus it has to exhibit a gradient in the surface layers.) Dölle, James and Cohen[5] have shown how to estimate the gradient using this curvature. It will be shown in this paper that, even for very small curvature in the "d" vs $\sin^2\psi$ data, analysis with the bi-axial assumption causes an appreciable error in the calculated surface stress. Methods are proposed that provide for the determination of the complete stress tensor in the surface layers in the

absence of ψ-splitting, i.e. when σ_{13}, σ_{23} are negligible. These methods are tested here by computer simulation.

THEORY

The orthogonal coordinate systems used in the following discussion are shown in figure 1. The specimen axes are defined such that $\underline{S}_1$ and $\underline{S}_2$ are in the surface of the sample. The laboratory system, in which diffraction is sampled, is defined such that $\underline{L}_3$ is in the direction of the normal to the family of planes (hkl) whose "d" spacings are being measured by x-rays. $\underline{L}_2$ is in the plane defined by $\underline{S}_1$ and $\underline{S}_2$, and makes an angle Φ with $\underline{S}_2$. In what follows, primed tensor quantities refer to the laboratory system $\underline{L}_i$ and unprimed quantities to the sample system $\underline{S}_i$, following the convention established by Dölle.[6]

If the unstressed lattice spacing "d_o" is known, strains in the $\underline{L}_3$ direction may be obtained from:

$$(\epsilon'_{33})_{\Phi,\psi} = \frac{d_{\Phi\psi} - d_o}{d_o} \quad . \tag{1}$$

This strain may be written in terms of strains in the $\underline{S}_i$ system of axes:[6]

$$(\epsilon'_{33})_{\Phi,\psi} = \epsilon_{11}\cos^2\Phi\sin^2\psi + \epsilon_{12}\sin 2\Phi\sin^2\psi + \epsilon_{22}\sin^2\Phi\sin^2\psi +$$

$$\epsilon_{33}\cos^2\psi + \epsilon_{13}\cos\Phi\sin 2\psi + \epsilon_{23}\sin\Phi\sin 2\psi \quad . \tag{2}$$

Expressing the strains on the right side of equation (2) in terms of stresses we obtain:

$$(\epsilon'_{33})_{\Phi,\psi} = \frac{1+\nu}{E}\left\{\sigma_{11}\cos^2\Phi + \sigma_{12}\sin 2\Phi + \sigma_{22}\sin^2\Phi - \sigma_{33}\right\}\sin^2\psi +$$

$$\left(\frac{1+\nu}{E}\right)\sigma_{33} - \frac{\nu}{E}(\sigma_{11} + \sigma_{22} + \sigma_{33}) + \frac{1+\nu}{E}\left\{\sigma_{13}\cos\Phi + \sigma_{23}\sin\Phi\right\}\sin 2\psi. \tag{3}$$

Here E is Young's modulus and ν is Poisson's ration. If a stress tensor of the form:

$$\sigma_{ij} = \begin{pmatrix} \sigma_{11} & o & o \\ o & \sigma_{22} & o \\ o & o & o \end{pmatrix} \tag{4}$$

exists in the volume sampled by the x-ray beam, equation (3) will yield the classical residual stress equation:

$$(\epsilon'_{33})_{\Phi,\psi} = \frac{1+\nu}{E}\left\{\sigma_{11}\cos^2\Phi + \sigma_{22}\sin^2\Phi\right\}\sin^2\psi - \frac{\nu}{E}(\sigma_{11} + \sigma_{22}) \ . \qquad (5)$$

Since $\sigma_{11}\cos^2\Phi + \sigma_{22}\sin^2\Phi \equiv \sigma_\Phi$(the stress in the direction $\underline{S}_\Phi$), equation (5) becomes:

$$(\epsilon'_{33})_{\Phi,\psi} = \frac{1+\nu}{E}\{\sigma_\Phi\}\sin^2\psi - \frac{\nu}{E}(\sigma_{11} + \sigma_{22}). \qquad (6)$$

It is seen from equations (6) and (1) that, the slope of "d" vs $\sin^2\psi$ is proportional only to σ_Φ when a bi-axial stress state is assumed. If a tri-axial stress tensor of the form:

$$\begin{pmatrix} \sigma_{11} & & 0 \\ & \sigma_{22} & \\ 0 & & \sigma_{33} \end{pmatrix} \qquad (7)$$

is present in the coordinate system $\underline{S}_i$, equation (3) becomes:

$$\langle\epsilon'_{33}\rangle_{\Phi,\psi} = \frac{1+\nu}{E}\{\sigma_{11}\cos^2\Phi + \sigma_{22}\sin^2\Phi - \langle\sigma_{33}\rangle_\psi\}\sin^2\psi + \left(\frac{1+\nu}{E}\right)\langle\sigma_{33}\rangle_\psi$$

$$- \frac{\nu}{E}\{\sigma_{11} + \sigma_{22} + \langle\sigma_{33}\rangle_\psi\} \ , \qquad (8a)$$

or:

$$\langle\epsilon'_{33}\rangle_{\Phi,\psi} = \frac{1+\nu}{E}\{\sigma_\Phi - \langle\sigma_{33}\rangle_\psi\}\sin^2\psi + \left(\frac{1+\nu}{E}\right)\langle\sigma_{33}\rangle_\psi$$

$$- \frac{\nu}{E}\{\sigma_{11} + \sigma_{22} + \langle\sigma_{33}\rangle_\psi\} \ , \qquad (8b)$$

where carats "$\langle\ \rangle$" imply averages over the depth of penetration of the X-ray beam.

From equations (8b) and (1) it can be seen that, when a stress tensor such as equation (7) exists in the surface layers, the slope of a linear least-squares fit to "d" vs $\sin^2\psi$ will be proportional to $\left[\sigma_\Phi - \langle\hat{\sigma}_{33}\rangle\right]$, where $\langle\hat{\sigma}_{33}\rangle$ is the normal stress averaged over the penetration depth (eqn. 26). Thus when $\langle\hat{\sigma}_{33}\rangle$ is present in the penetrated volume, there will be an error

in the stress σ_Φ, determined from the slope by the conventional (bi-axial) analysis, equal in magnitude to $\langle\widehat{\sigma_{33}}\rangle$.

It is possible to obtain both $\langle\sigma_{33}\rangle$ and σ_Φ using equations (8b) and (1). There are a total of three unknowns: Stresses σ_Φ, $\langle\sigma_{33}\rangle$ and the angle Φ, which is the angle between the principal axis $\underline{S}_1$ and the measurement direction $\underline{S}_\Phi$. A simple method of determining the stresses $\langle\sigma_{33}\rangle$ and σ_Φ is presented below.

If data for "d vs $\sin^2\psi$ is obtained at two Φ angles; Φ_A and $\Phi_A + 90^\circ$, where Φ_A is arbitrary, the slopes of "d" vs $\sin^2\psi$, M_{Φ_A}, $M_{\Phi_A+90^\circ}$ will be:

$$M_{\Phi_A} = \left(\frac{1+\nu}{E}\right)\left\{\sigma_{11}\cos^2\Phi_A + \sigma_{22}\sin^2\Phi_A - \langle\widehat{\sigma_{33}}\rangle\right\} \tag{9a}$$

$$= \left(\frac{1+\nu}{E}\right)\left\{\sigma_{\Phi_A} - \langle\widehat{\sigma_{33}}\rangle\right\} . \tag{9b}$$

$$M_{\Phi_A+90^\circ} = \left(\frac{1+\nu}{E}\right)\left\{\sigma_{11}\cos^2(\Phi_A+90^\circ) + \sigma_{22}\sin^2(\Phi_A+90^\circ) - \langle\widehat{\sigma_{33}}\rangle\right\} \tag{9c}$$

$$= \left(\frac{1+\nu}{E}\right)\left\{\sigma_{\Phi_A+90^\circ} - \langle\widehat{\sigma_{33}}\rangle\right\} . \tag{9d}$$

Summing Eqns. (9a) and (9c) we obtain:

$$M_{\Phi_A} + M_{\Phi_A+90^\circ} = \left(\frac{1+\nu}{E}\right)\left\{\sigma_{11} + \sigma_{22} - 2\langle\widehat{\sigma_{33}}\rangle\right\} , \tag{10a}$$

or;
$$(\sigma_{11} + \sigma_{22}) = \left(\frac{E}{1+\nu}\right)\left\{M_{\Phi_A} + M_{\Phi_A+90^\circ}\right\} + 2\langle\widehat{\sigma_{33}}\rangle . \tag{10b}$$

The intercept I of $\langle\epsilon'_{33}\rangle$ in Eqn. 8a vs $\sin^2\psi$ at $\psi=0^\circ$ does not depend on Φ,

$$I = \left(\frac{1+\nu}{E}\right)\langle\widehat{\sigma_{33}}\rangle - \frac{\nu}{E}\langle\widehat{\sigma_{33}}\rangle - \frac{\nu}{E}(\sigma_{11} + \sigma_{22}) . \tag{11}$$

The constants $\left(\frac{1+\nu}{E}\right)$ and $-\frac{\nu}{E}$ are "X-ray elastic constants" and may be obtained from the literature for a given reflection, hkl, and material, or

measured following the procedures outlined in reference 7. (Since only slopes of load vs "d" are used in these procedures, effect of gradients are eliminated.) Equations (11) and (10b) are then solved simultaneously for $\langle\hat{\sigma}_{33}\rangle$ and $(\sigma_{11}+\sigma_{22})$. With $\langle\hat{\sigma}_{33}\rangle$, the stresses in $\underline{S}_{\Phi_A}$ and $\underline{S}_{\Phi_A+90^\circ}$ directions, σ_{Φ_A} and $\sigma_{\Phi_A+90^\circ}$, are obtained from equations (9b) and (9d) respectively.

The analysis described here yields the stress normal to the surface; $\langle\hat{\sigma}_{33}\rangle$, and two stresses in the surface plane; σ_{Φ_A} and $\sigma_{\Phi_A+90^\circ}$. It is also possible to obtain the first stress invariant $I_1=\sum_{i=1}^{3}\sigma_{ii}$. If the principal stresses in the surface σ_{11}, σ_{22} and the angle Φ these form with the measurement direction $\underline{S}_\Phi$ are required, "d" vs $\sin^2\psi$ values must be obtained for a third Φ angle, $\Phi_A+\alpha$, where α is arbitrary ($\alpha \neq 90^\circ$) The slope of the "d" vs $\sin^2\psi$ line, $M_{\Phi_A+\alpha}$ will be:

$$M_{\Phi_A+\alpha} = \frac{1+\nu}{E}\left\{\sigma_{11}\cos^2(\Phi_A+\alpha) + \sigma_{22}\sin^2(\Phi_A+\alpha) - \langle\sigma_{33}\rangle\right\} . \qquad (12)$$

Since $\langle\hat{\sigma}_{33}\rangle$ is known, σ_{11}, σ_{22} and Φ may be obtained by simultaneously solving equations (9a), (9c) and (12).

Special Case

Some important surface treatments such as shot peening produce residual stresses which are isotropic in the surface. The stress tensor is then of the form:

$$\sigma_{ij} = \begin{pmatrix} \sigma_{11} & & \delta \\ & \sigma_{11} & \\ \delta & & \sigma_{33} \end{pmatrix} \quad (13), \text{ where } \delta \ll \sigma_{ij} .$$

For such cases, the analysis is simplified and the time of measurement is reduced. Substituting equation (13) into equation (3):

$$(\epsilon'_{33})_\psi = \left(\frac{1+\nu}{E}\right)\left\{\sigma_{11} - \langle\sigma_{33}\rangle_\psi\right\}\sin^2\psi + \left(\frac{1+\nu}{E}\right)\langle\sigma_{33}\rangle$$

$$- \frac{\nu}{E}\left\{\langle\sigma_{33}\rangle_\psi + 2\sigma_{11}\right\} \qquad (14)$$

Since the slope and intercept of "$(\epsilon'_{33})_\psi$" vs $\sin^2\psi$ may be solved for σ_{11} and $\langle\sigma_{33}\rangle$, one arbitrary ψ tilt is sufficient to obtain the complete stress tensor in the surface layers sampled by the x-ray beam. In other words, the usual measurement of "d" vs $\sin^2\psi$ suffices, but the slope and the intercept at $\psi = 0^o$ must be employed.

Effect of Curvature

The term "σ_{33}", used in the previous equations, is a stress normal to the surface. It is, of course, exactly zero at the surface. Therefore σ_{33} can exist only as a gradient in the near surface layers. It is well known that, when such stress gradients are present, curvature occurs in the "d" vs $\sin^2\psi$ plots[3,5,6], and, as mentioned above, a method has been proposed to use this curvature to obtain the gradient.[5] It has also been suggested that the slope of a linear least-squares fit will yield an "average" value of the stress state over the depth of penetration.[3] Since the x-ray beam penetrates to different depths at each ψ-tilt, a different portion of the existing gradient is sampled with each ψ-tilt, causing the curvature in "d" vs $\sin^2\psi$. Analysis of such data by linear least-squares may cause appreciable error in the slope and intercept of the line fitted to the data. This error is now examined.

We assume that the behavior of stress, σ_{ij}, with depth follows a power law*:

$$\sigma_{ij}(z) = \sigma_{ij}(z = 0) + a_{ij} z^{n_{ij}} , \qquad (15)$$

Where $\sigma_{ij}(z = 0)$ is the stress value at the surface, a_{ij}, n_{ij} are constants (over the depth of penetration) and z is the distance coordinate along the normal to the surface (measured into the material).

The average stress obtained by x-rays penetrating to a depth "z" is:[6]

$$\langle\sigma_{ij}\rangle_z = \frac{\int_0^\infty \sigma_{ij} e^{-z/\tau} dz}{\int_0^\infty e^{-z/\tau} dz} \qquad (16)$$

*For example, in case of autofrettage, (shrink-fitting of cylinders on solid shafts), $n_{ij} = 2$ for tangential and radial stresses.[9]

where τ is given by:[7]

$$\tau_{\Omega} = \frac{\sin^2\theta - \sin^2\psi}{2\mu\sin\theta\cos\psi} \quad , \tag{17a}$$

for ψ tilts around the θ axis and

$$\tau_{\psi} = \frac{\sin\theta\cos\psi}{2\mu} \quad , \tag{17b}$$

for tilts around an axis parallel to the diffractometer plane. Here μ is the linear absorbtion coefficient, θ the Bragg angle of diffraction and ψ is defined in figure 1. Variation of τ_{Ω} and τ_{ψ} with ψ are shown in figure 2.

Substituting equation (15) into equation (16) and integrating:

$$\langle \sigma_{ij} \rangle_{\psi} = \sigma_{ij}(z=0) + K_{ij}\tau^{n}{}_{ij} \tag{18}$$

Where K_{ij} is a constant, n_{ij} is the exponent of the stress variation (Eqn. 15) and τ is given by equations 17.

Assume, for simplicity, that a stress tensor of the form given in equation (13) exists in the near surface layers and that the stress in the surface plane σ_{11} is not dependent on depth. For σ_{33}, equation (18) becomes:

$$\langle \sigma_{33} \rangle_{\psi} = K_{33}\tau^{n}33 \qquad (19), \text{ where } n_{33} \neq 0 \ .$$

Substituting equation (19) into equation (14) and re-arranging:

$$\frac{d_{\phi,\psi} - d_o}{d_o} = \langle \epsilon'_{33} \rangle_{\psi} = \left(\frac{1+\nu}{E}\right)\sigma_{11}\sin^2\psi - \frac{2\nu}{E}\sigma_{11} + \frac{K_{33}\tau^{n}33}{E}\{(1+\nu)(1-\sin^2\psi) - \nu\} \tag{20}$$

The equation of a least-squares line is:[8]

$$Y = \beta_o + \beta_1 X + e \ , \tag{21}$$

where Y: the dependent variable

X: the independent variable

e: error

β_o, β_1: regression parameters.

Comparing equations (6), (20) and (21), we observe that, if a least-squares line is assumed, (i.e. assuming only a bi-axial stress state), the error term will be:

$$e_{\psi} = \frac{K_{33}\tau^{n}33}{E}\{(1+\nu)(1-\sin^2\psi) - \nu\} \ . \tag{22}$$

It is seen from equation (22) that:

i) e_{ψ} is a biased error. (It is systematic.)

ii) For a fixed depth (fixed ψ), the error "e_ψ" in $(\epsilon'_{33})_\psi$ increases with increasing exponent of the stress (n_{33}).

iii) For a fixed n_{33}, there will be greater bias in $(\epsilon'_{33})_\psi$ measured at low ψ (high τ) tilts than for $(\epsilon'_{33})_\psi$ measured at high ψ (low τ) angles.

Analysis of data corresponding to equation (20) by conventional methods ignores the error components, e_ψ, associated with each point and forces a linear least-squares solution to the data. Since the error is not random, but highly biased, such a procedure may yield large errors in the stress calculated from the slope, which depend on a_{33}, n_{33} in equation (15).

When a tri-axial stress state, (Eqn. 14), is employed, there will still be some error due to this curvature; expanding equation (20):

$$\langle\epsilon'_{33}\rangle_\psi = \left(\frac{1+\nu}{E}\right)\left\{\sigma_{11} - K_{33}\tau^{n_{33}}\right\}\sin^2\psi + \left(\frac{1+\nu}{E}\right)K_{33}\tau^{n_{33}} - \frac{\nu}{E}\left\{K_{33}\tau^{n_{33}} + 2\sigma_{11}\right\} \qquad (23)$$

A least-squares fit to the data (with equation 14) yields the equation:

$$\langle\epsilon'_{33}\rangle_\psi = \left(\frac{1+\nu}{E}\right)\{\sigma_{11} - \langle\hat{\sigma}_{33}\rangle\}\sin^2\psi + \left(\frac{1+\nu}{E}\right)\langle\hat{\sigma}_{33}\rangle - \frac{\nu}{E}\{\langle\hat{\sigma}_{33}\rangle + 2\sigma_{11}\}\ , \qquad (24)$$

Thus, the deviation of each point $\langle\epsilon'_{33}\rangle_\psi$ from linearity is:

$$e'_\psi = \frac{(K_{33}\tau^{n_{33}} - \langle\hat{\sigma}_{33}\rangle)}{E}\{(1+\nu)(1-\sin^2\psi) + \nu\}\ , \qquad (25)$$

where $\langle\hat{\sigma}_{33}\rangle$ is the least-squares average of $\langle\sigma_{33}\rangle_\psi$ values*

---

*The equation for $\langle\hat{\sigma}_{33}\rangle$ is:

$$\langle\hat{\sigma}_{33}\rangle = \sigma_{11} - \frac{\sum_{i=1}^{N}(X_i - \bar{X})(Y_i - \bar{Y})}{\sum_{i=1}^{N}(X_i - \bar{X})^2} \cdot \frac{E}{(1+\nu)} \qquad (26)$$

where $X = \sin^2\psi$

$Y = \langle\epsilon'_{33}\rangle_\psi$, N = Number of ψ-tilts and $\bar{X} = \left(\sum_{i=1}^{N} X_i\right)/N$, $\bar{Y} = \left(\sum_{i=1}^{N} Y_i\right)/N$

We see that the normal stress obtained from the slope, $\langle\hat{\sigma}_{33}\rangle$, is a double average; first averages are taken by x-rays over different regions of the stress gradient, than these are averaged again by the least-squares fitting.

Comparing equations (25) and (22) we observe that, while the absolute magnitude of bias associated with a given $(\epsilon'_{33})_\psi$ is less when the tri-axial analysis is used, some error will remain, causing an error in stresses calculated from the slope and intercept of the "d" vs $\sin^2\psi$ data. These errors will be termed "curvature errors" here. It is seen from equation (25) that, for high ψ angles (low penetration depths), the bias associated with $(\epsilon'_{33})_\psi$ will be smaller than for low ψ points. Thus a least-squares analysis of the high ψ range will produce a more meaningful fit of the linear model to the data, in the presence of such curvature.

General Case

Up to this point it has been assumed that, no shear stresses in the direction of the surface normal exist. This assumption is not necessary as far as the curvature error is concerned. When a general stress state is present in the near-surface layers, the strains in the $(\underline{L}_3)_{\Phi,\psi}$ direction are given by equation 3. The analysis in this case has been described by Dölle.[6] The quantities a_1, a_2 are formed:

$$a_1 = \tfrac{1}{2}(\epsilon'_{\Phi\psi+} + \epsilon'_{\Phi\psi-}) = \left(\frac{1+\nu}{E}\right)\{\sigma_{11}\cos^2\Phi + \sigma_{12}\sin 2\Phi + \sigma_{22}\sin^2\Phi - \langle\sigma_{33}\rangle_\psi\} \cdot$$

$$\sin^2\psi + \left(\frac{1+\nu}{E}\right)\langle\sigma_{33}\rangle_\psi - \frac{\nu}{E}(\sigma_{11} + \sigma_{22} + \langle\sigma_{33}\rangle_\psi), \qquad (27a)$$

$$a_2 = \tfrac{1}{2}(\epsilon'_{\Phi\psi+} - \epsilon'_{\Phi\psi-}) = \left(\frac{1+\nu}{E}\right)\{\langle\sigma_{13}\rangle_\psi\cos\Phi + \langle\sigma_{23}\rangle_\psi\sin\Phi\}\sin|2\psi|, \qquad (27b)$$

Where $\epsilon'_{\Phi\psi+}$ is the ϵ'_{33} measured at $\psi = +\psi$ and Φ, and $\epsilon'_{\Phi\psi-}$ is the ϵ'_{33} measured at $\psi = -\psi$, and Φ.

It is seen that, a_1 and a_2 will have curvature when plotted against $\sin^2\psi$ and $\sin|2\psi|$ respectively, since both contain components that are a function of depth $(\sigma_{3j,j=1,3})$. In fact a_1 (Eqn. 27a) is a general form of Eqn. (24). Using high ψ-points to form the arrays a_1 vs $\sin^2\psi$ and a_2 vs $\sin|2\psi|$ will minimize the curvature error associated with this analysis.

If gradients are present in all components of a general stress tensor, equations (20) - (25) will have additional terms. However the general ideas discussed above will still be valid for most cases.

DATA SIMULATION AND ANALYSIS

Computer simulation of "d" vs $\sin^2\psi$ was used to obtain information about the magnitudes of errors, resulting from the presence of $\langle\hat{\sigma}_{33}\rangle$ and the curvature error. A computer program was written which calculated the strains in the $\underline{S}_i$ coordinate system for a given stress tensor, converted these strains into strains in the $(\underline{L}_3)_{\Phi,\psi}$ direction and formed the "d" vs $\sin^2\psi$ array for a given Φ. The generated, ϵ'_{33}, vs $\sin^2\psi$ were then analyzed by the methods described above.

Three different stress-tensor groups were investigated. The assumptions common to all three groups are:

1) The hypothetical sample is steel.

2) Cr radiation is used in the analysis. The ψ-goniometer geometry is assumed.

3) Elastic constants do not change with depth.

4) The constants a_{ij}, n_{ij}, defined by equation (15) are constant over the maximum depth of penetration (5.4μ).

5) For simplicity, it was assumed that the stress state in the plane of the surface is isotropic ($\sigma_{11} = \sigma_{22}$) and the variation of σ_{11} and σ_{22} with depth are identical:

$$\frac{\partial\sigma_{11}}{\partial z} = \frac{\partial\sigma_{21}}{\partial z} \quad .$$

Here, $(\sigma_{11})_{z=0}$ was chosen arbitrarily as -400 MPa.

6) Different exponents (n_{33}) were used to form the $\langle\sigma_{33}\rangle_\psi$ profiles with depth. However, in all cases K_{33} values were selected such that $\langle\hat{\sigma}_{33}\rangle$ (Eqns. 24,26) was approximately 100 MPa. This value was chosen

since experimental values reported in literature on steels are generally between 80 - 140 MPa.[4,5]

7) For a given stress tensor, the ϵ'_{33} vs $\sin^2\psi$ array was examined as follows:

a. Bi-axial analysis (Eqn. 6) over the entire ψ-range, $\psi\epsilon(0^\circ, 60^\circ)$, and, only over the high ψ-range, $\psi\epsilon(45,60)$.

b. Two tilt* analysis using $\psi = 0$ and 45°, and 0 and 60°, and 45° and 60° respectively.

c. Tri-axial analysis (Eqn. 24) over the entire ψ-range.

d. Tri-axial analysis over $\psi = (0, 33.21^\circ)$; first four points.

e. Tri-axial analysis over $\psi = (39.23 - 60^\circ)$; last four points.

8) The results are shown in tables (1-3) which show the ψ-range employed, the stress exponents (n_{ij}) assumed to exist in the penetration volume, type of analysis used to obtain the stresses σ_{ij}, the error resulting from the analysis, the type of error and the correlation coefficient of the regression line fitted to the "d" vs $\sin^2\psi$ data.

Group I

For this group, σ_{11}, σ_{22} were assumed to be constant over the depth of penetration. Three types of gradients were assumed for σ_{33}, with the stress exponent $n_{33} = 1,2,3$ respectively. The $\langle\sigma_{33}\rangle_\psi$ profiles with depth (Eqn. 19) for each case are shown in figure 3a. For all three cases the average value $\langle\hat{\sigma}_{33}\rangle$ (Eqns. 24,26) is approximately 100 MPa, although the gradient is much steeper for $n_{33} = 3$ compared to the gradient for $n_{33} = 1$.

The stress tensor sampled by the x-ray beam at any ψ-tilt will be :

$$\langle\sigma_{ij}\rangle_\psi = \begin{pmatrix} -400 & & 0 \\ & -400 & \\ 0 & & \langle\sigma_{33}\rangle_\psi \end{pmatrix} . \qquad (28)$$

*In "two-tilt" analysis, it is assumed that all "d" vs $\sin^2\psi$ values fall on a straight line.[1] Thus only the first and last data points are used to obtain the stress.

The "d" vs $\sin^2\psi$ plots corresponding to stress tensor (28) for different n_{33} values are shown in figure 3b. It is seen that:

i) Curvature in "d" vs $\sin^2\psi$ increases with increasing exponent n_{33}.

ii) All three curves converge as $\sin^2\psi$ increases, (penetration depth decreases) as the gradients in stress also converge.

Analysis for all three cases (n_{33} = 1,2,3) are summarized in table I. Examination of this table reveals that:

1) If a bi-axial assumption is used in analyzing "d" vs $\sin^2\psi$ data obtained from surface layers, when a tri-axial stress tensor is present, appreciable error will occur in the stress value calculated from the slope. The error will be the sum of two components:

i) The $\langle\hat{\sigma}_{33}\rangle$ value that will contribute directly to the slope (Eqn. 24).

ii) The curvature error which arises from fitting a least-squares line to curved data.

2) If a tri-axial solution is used (Eqn. 24), the σ_{11} calculated from the slope will be corrected for $\langle\hat{\sigma}_{33}\rangle$, but the curvature error remains.

3) Curvature error increases with increasing n_{33}, as predicted by eqn. 25 and may be quite high if a low ψ range is used.

4) The curvature error is minimized if a least-squares line is fitted to high ψ points only. This effect is due to decreasing absolute error, associated with high ψ points, as predicted by equation (25).

It can be seen from equation(25) that, when no gradients are present in σ_{11} and σ_{22}, curvature error is only a function of the σ_{33} gradient. It is not dependent on the magnitude of σ_{11}. In figure 4, the variation of curvature error with magnitude of $\langle\hat{\sigma}_{33}\rangle$ is plotted for n_{33} = 1,2,3 respectively, when a high ψ range ($\psi\epsilon 39.23\text{-}60^\circ$) is used. Also included, as a basis for comparison, is the total error in the stress obtained from a bi-axial analysis using the total ψ-range (0, 60°) for the same $\langle\hat{\sigma}_{33}\rangle$ values (n_{33} = 1 for this case). It is seen that, using tri-axial analysis over the high ψ-range will result in a maximum curvature error of 25 MPa (for $\langle\hat{\sigma}_{33}\rangle$ < 170 MPa) which is generally within the total experimental error.

Groups II and III

To check the generality of the conclusions arrived at in group I, the effects of stress gradients in other terms of the stress tensor were investigated:

In group II, a stress tensor of the form,

$$(\sigma_{ij})_\psi = \begin{pmatrix} \langle\sigma_{11}\rangle_\psi & & 0 \\ & \langle\sigma_{11}\rangle_\psi & \\ 0 & & 0 \end{pmatrix} , \qquad (29)$$

was assumed, where $\langle\sigma_{11}\rangle = -400 + K_{11}z^2$ MPa.

The calculated stress profile with depth for this case is shown in figure 5a, with the resulting "d" vs $\sin^2\psi$ in figure 5b. The curvature agrees with that calculated by Dölle et al. However high ψ values are needed to see the effect, since the gradient is not very steep compared to those in figure 3a.

Results of analysis are shown in table II. The $\langle\hat{\sigma}_{33}\rangle$ values obtained in this case are residuals due to misfit of the linear regression equation. When a high ψ-range is used, the residual is well within experimental error. It is seen that, whereas analysis of tri-axial data by bi-axial methods yields very high error, analysis of bi-axial data by tri-axial methods is more accurate, especially if the high ψ-range is employed.

In group III the effect of combined gradients were examined. Gradients were assumed in all components of the stress tensor (13). Two cases were examined:

a) $\langle\sigma_{11}\rangle_\psi = -400 + K_{11}z$, where $K_{11} = 5$ MPa/μ

$\langle\sigma_{33}\rangle_\psi = K_{33}z^2$

b) $\langle\sigma_{11}\rangle_\psi = -400 + K_{11}z^2$

$\langle\sigma_{33}\rangle_\psi = K_{33}z^2$

The calculated stress profiles for both cases are shown in figures (6a) and (6b) respectively. The resultant "d" vs $\sin^2\psi$ graphs are shown in figure (6c). Again both lines converge for high ψ angles. The results of analysis are summarized in table III.

Examination of tables II and III show that the conclusions from group I are indeed general. It can also be seen that a high correlation coefficient in "d" vs $\sin^2\psi$ is not a good measure of the dimensionality of the stress tensor.

Summary

1) Deviations of interplanar spacing "d" vs $\sin^2\psi$ from linearity, arising from stress gradients are generally small, confirming previous comments on this matter.(5)

2) Analysis of even slightly curved "d" vs $\sin^2\psi$ plots assuming a bi-axial surface stress state may cause high error in the stress value determined from the slope.

3) Employing the methods for tri-axial stress tensors described here will minimize errors due to the average value of the stress normal to the surface. There will, however, still be some residual error associated with curvature of the data.

4) This curvature error may be minimized by using high ψ points in the linear least-squares fit, ($\sin^2\psi > .4$).

5) When two radiations are available for a measurement, the one having a high absorbtion coefficient (low penetration depth) should be used if stress gradients with depth are present. This will also minimize errors due to curvature.

6) Unless it is absolutely clear that stresses normal to the surface are absent, or quite small, the current x-ray method of stress analysis should be replaced by the methods described here.

ACKNOWLEDGEMENTS

The author wishes to thank Prof. J. B. Cohen for extensive discussions and suggestions on this paper. Prof. J. W. Ho also reviewed the manuscript and made many relevant suggestions. The work was supported by ONR under contract No. N00014-80-C-0116. Thanks are also due to Turkish Scientific and Technical Research Council for supplying a NATO grant, which enabled the author to study in USA.

REFERENCES

1. B. D. Cullity: Elements of X-ray Diffraction, 2nd ed., pp. 447-79, Addison-Wesley, Reading, MA, 1978.
2. C. S. Barrett and T. B. Massalski: Structure of Metals, 3rd ed., pp. 465-85, McGraw-Hill, New York, 1966.
3. T. Shiraiwa and Y. Sakamoto: Sumito Search, 1972, Vol. 7, pp. 159-169.
4. H. Dölle and J. B. Cohen: Met. Trans. A, 1980, Vol. 11A, pp. 159-169.
5. J. B. Cohen, H. Dölle and M. R. James: National Bureau of Standards Special Publication 567, 1980, pp. 453-477.
6. H. Dölle: J. Appl. Cryst., 1979, Vol. 12, pp. 489-501.
7. C. J. Kelley and A. M. Short: SAE Technical Report J784a, 1971, pp. 61-62.
8. N. R. Draper and H. Smith: Applied Regression Analysis, 1st ed., pp. 1-43, Wiley- Interscience, New York, 1966.
9. S. P. Timoshenko and J. N. Goodier: Theory of Elasticity, 3rd ed., P, 71, McGraw-Hill, New York, 1970.

TABLE TITLES

Table I: Analysis of "d" vs $\sin^2\psi$ plots I-1, I-2, I-3, in figure 3b.*

Table II: Analysis of "d" vs $\sin^2\psi$ shown in figure 5b.**

Table III: Analysis of "d" vs $\sin^2\psi$ plots III-1, III-2, shown in figure 6b.***

---

* For all cases σ_{11}° is -400 MPa $\langle\sigma_{33}\rangle$ values shown are average values; σ_{33} is zero at the surface z=0. The gradient in $\langle\sigma_{33}\rangle_{\psi}$ is shown in figure 3a for all three cases, n_{33}=1,2,3.

** $\sigma_{11}^{\circ} = \sigma_{11}(z=0)$ is -400 MPa and $\sigma_{33}(z)=0$. The $\langle\sigma_{33}\rangle$ values obtained from the analysis are residual errors due to the misfit of the linear model used in analysis.

***In this case there are gradients in both σ_{11} and σ_{33}, (figure 6a). $\sigma_{11}^{\circ} = \sigma_{11}(z=0)$ = -400 MPa and $\sigma_{33}(z=0) = 0$.

TABLE I

ψ-Range (Degrees)	n_{33}	Type of Analysis	$\langle\hat{\sigma}_{11}\rangle$ (MPa)	$\langle\hat{\sigma}_{33}\rangle$ (MPa)	Error in $\langle\hat{\sigma}_{33}\rangle$ $\lvert\langle\hat{\sigma}_{11}\rangle-\sigma_{11}^{\circ}\rvert$	Type of error in $\hat{\sigma}_{11}$	Correlation Coefficient of "d"vs $\sin^2\psi$ plot
0-45	1	Bi-axial "two-tilt"	-553.6	0	153.6	$\langle\hat{\sigma}_{33}\rangle$ + Curvature	
0-60	1	"	-535.8	0	135.8	"	
45-60	1	"	-499.4	0	99.4	"	
0-60	1	Bi-axial "$\sin^2\psi$"	-537.14	0	137.14	"	-.9995
45-60	1	"	-500.5	0	100.5	"	-.9999
0-60	1	Triaxial	-428.19	108.96	28.19	Curvature	-.9995
0-33.21	1	"	-500.14	68.17	100.14	"	-.9998
39.23-60	1	"	-404.72	99.30	4.72	"	-.9997
0-45	2	Bi-axial "Two-Tilt"	-618.8	0	218.8	$\langle\hat{\sigma}_{33}\rangle$ T Curvature	
0-60	2	"	-579.0	0	179.0	"	
45.60	2	"	-499.4	0	99.4	"	
0-60	2	Bi-axial "$\sin^2\psi$"	-577.81	0	177.81	"	-.9977
45-60	2	"	-500.5	0	100.5	"	-.9999
0-60	2	Tri-axial	-461.96	115.85	61.96	Curvature	-.9977
0-33.21	2	"	-639.72	14.66	239.72	"	-.9993
39.23-60.	2	"	-408.69	95.08	8.69	"	-.9997
0-45	3	Bi-axial "Two-Tilt"	-705.60	0	305.60	$\langle\hat{\sigma}_{33}\rangle$ T Curvature	
0-60	3	"	-636.90	0	236.90	"	
45-60	3	"	-493.4	0	93.4	"	
0-60	3	Bi-axial "$\sin^2\psi$"	-637.89	0	237.89	"	-.9938
45-60	3	"	-496.6	0	96.6	"	-.9993
0-60	3	Tri-axial	-507.59	130.31	107.59	Curvature	-.9938
0-33.21	3	"	-849.15	-64.89	449.15	"	-.9988
39.23-60	3	"	-412.55	95.22	12.55	"	-.9993

TABLE II

ψ-Range (Degrees)	n_{11}	Type of Analysis	$\langle\hat{\sigma}_{11}\rangle$ (MPa)	$\langle\hat{\sigma}_{33}\rangle$ (MPa)	Error in $\langle\hat{\sigma}_{11}\rangle$ $\lvert\langle\hat{\sigma}_{11}\rangle - \sigma_{11}^{o}\rvert$	Type of Erron in σ_{11}	Correlation Coefficient of "d" vs $\sin^2\psi$ plot.
0-45	1	Bi-axial "Two-Tilt"	-336.4	0	63.6	Curvature	
0-60	1	"	-354.5	0	45.5	"	
45.60	1	"	-361.8	0	38.2	"	
0-60	1	Bi-axial "$\sin^2\psi$"	-355.66	0	44.34	"	-.9993
45-60	1	"	-415.8	0	15.8	"	-.9987
0-60	1	Tri-axial	-364.86	-9.20	35.14	"	-.9993
0-33.21	1	"	-305.60	24.53	94.40	"	-.9999
39.23-60	1	"	-382.61	-2.272	17.39	"	-.9986

TABLE III

ψ-range (Degrees)	n_{11}	n_{33}	Type of Analysis	$\langle\hat{\sigma}_{11}\rangle$ (MPa)	$\langle\hat{\sigma}_{33}\rangle$ (MPa)	Error in σ_{11} $\lvert\langle\sigma_{11}\rangle - \sigma_{11}^{\circ}\rvert$	Type of error in σ_{11}	Correlation Coefficient of "d" vs $\sin^2\psi$ plot.
0-45	1	2	Bi-axial "Two-Tilt"	-575.5	0	175.5	$\langle\hat{\sigma}_{33}\rangle$ + Curvature	
0-60	1	2	"	-535.7	0	135.7	"	
45-60	1	2	"	-456.0	0	56.0	"	
0-60	1	2	Bi-axial "$\sin^2\psi$"	-540.08	0	140.08	"	-.9982
45-60	1	2	"	-458.4	0	58.4	"	-.9996
0-60	1	2	Tri-axial	-436.90	103.20	36.90	Curvature	-.9962
0-33.21	1	2	"	-583.70	19.57	183.70	"	-.9999
39.23-60	1	2	"	-393.39	86.36	6.61	"	-.9992
0-45	2	2	Bi-axial "Two-Tilt"	-586.1	0	186.1	$\langle\hat{\sigma}_{33}\rangle$ T Curvature	
0-60	2	2	"	-550.0	0	150.0	"	
45-60	2	2	"	-477.6	0	77.6	"	
0-60	2	2	Bi-axial "$\sin^2\psi$"	-548.29	0	148.29	"	-.9985
45-60	2	2	"	-477.3	0	77.3	"	-.9999
0-60	2	2	Tri-axial	-431.98	116.31	31.98	Curvature	-.9985
0-33.21	2	2	"	-565.30	40.42	165.30	"	-.9997
39.23-60	2	2	"	-392.02	100.73	7.98	"	-.9995

FIGURE CAPTIONS

Figure 1 : Definition of the angles ϕ and ψ and orientation of the laboratory system $\underline{L}_i$ with respect to the sample system $\underline{S}_i$ and the measurement direction $\underline{S}_\phi$.

Figure 2 : Penetration depth "T" vs $\sin^2\psi$ for Cr-radiation on steel at $2\theta = 156^\circ$.

Figure 3a: Calculated $\langle\sigma_{33}\rangle_\psi$ profiles vs depth for group I. In all three cases $\sigma_{11} = \sigma_{22} = -400$ MPa throughout the depth of penetration.

Figure 3b: The "d" vs $\sin^2\psi$ corresponding to the stress profiles shown in figure 3a. (The results of analysis for these curves are shown in Table I, groups I-1, I-2, I-3 respectively.)

Figure 4 : Variation of the magnitude of error in the surface stress σ_{11} with the magnitude of the average stress in the direction of the surface normal. The steepest curve shows the error in surface stress determined by bi-axial analysis for $\psi = 0\text{-}60^\circ$. The other three curves show errors resulting from triaxial analysis for $\psi = 39.23 - 60^\circ$.

Figure 5a: Residual-stress profile vs depth for group II. In this case there is no stress gradient in the direction of the surface normal.

Figure 5b: The "d" vs $\sin^2\psi$ plot corresponding to the stress profile with depth shown in figure 5a. Results of analysis of this curve are summarized in Table II.

Figure 6a: Residual stress profiles with depth for group III-1.

Figure 6b: Residual stress profiles with depth for group III-2.

Figure 6c: The "d" vs $\sin^2\psi$ corresponding to residual stress profiles shown in figures 6a and 6b. The results of analysis for both curves are summarized in Table III, groups III-1, III-2 respectively.

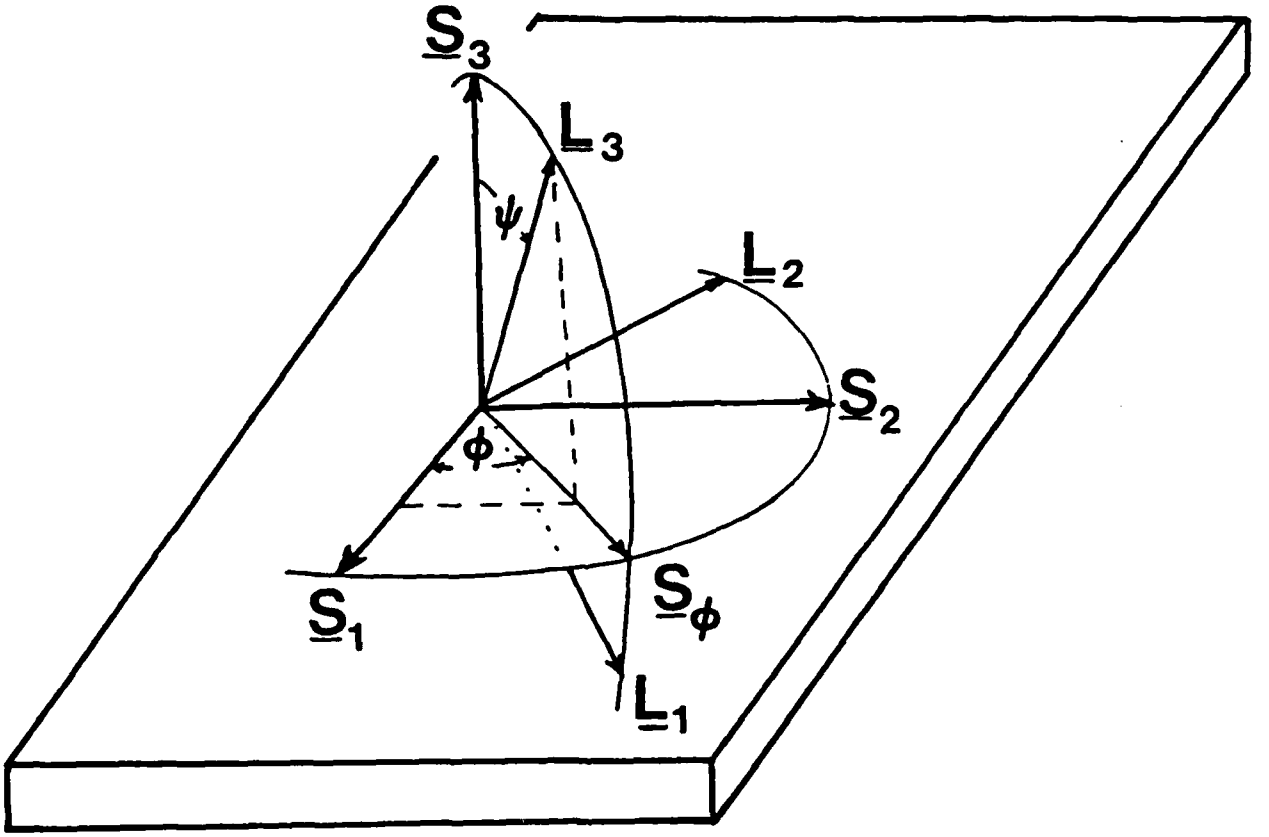

FIGURE 1

I. C. Noyan

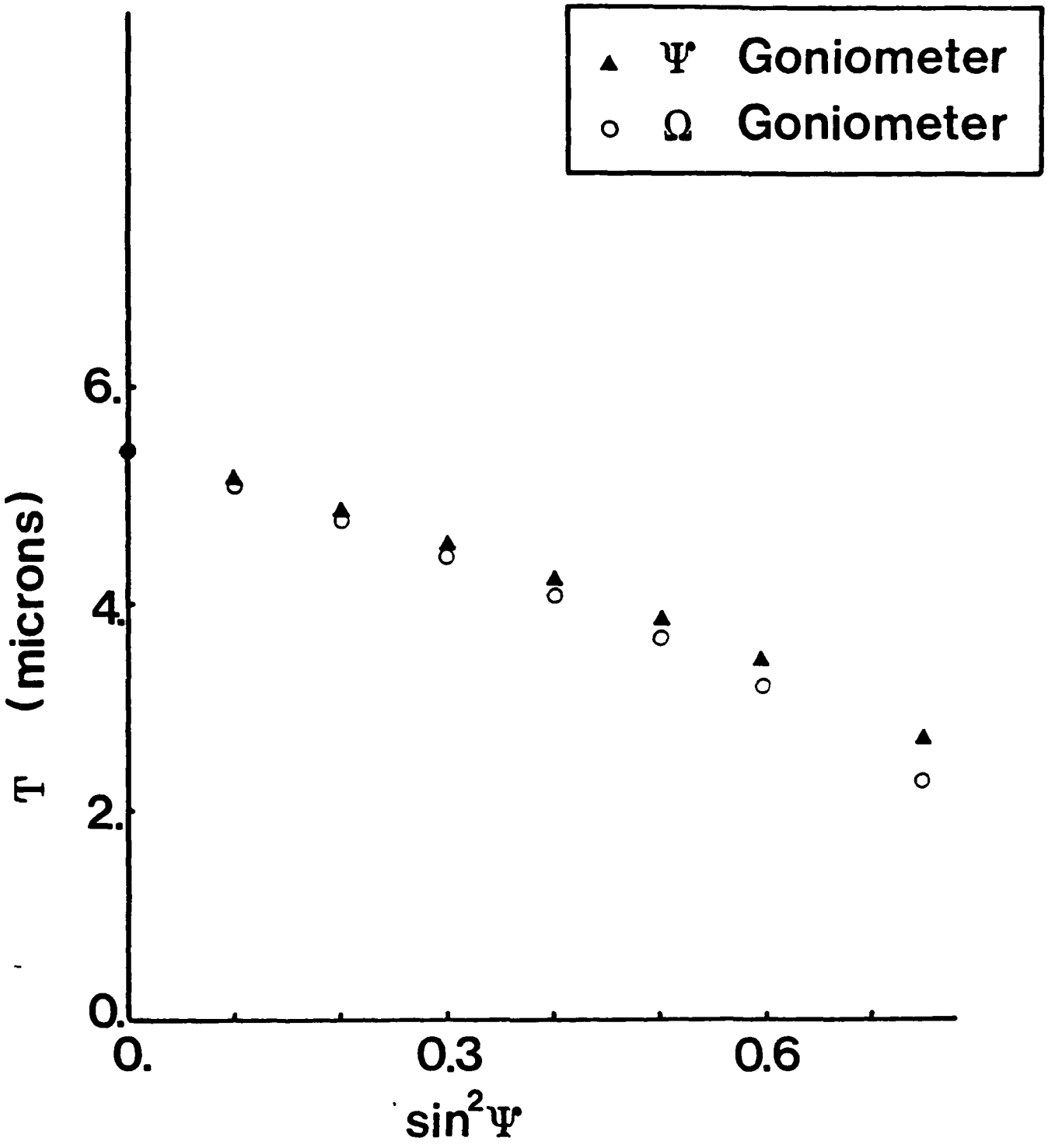

FIGURE 2

I. C. Noyan

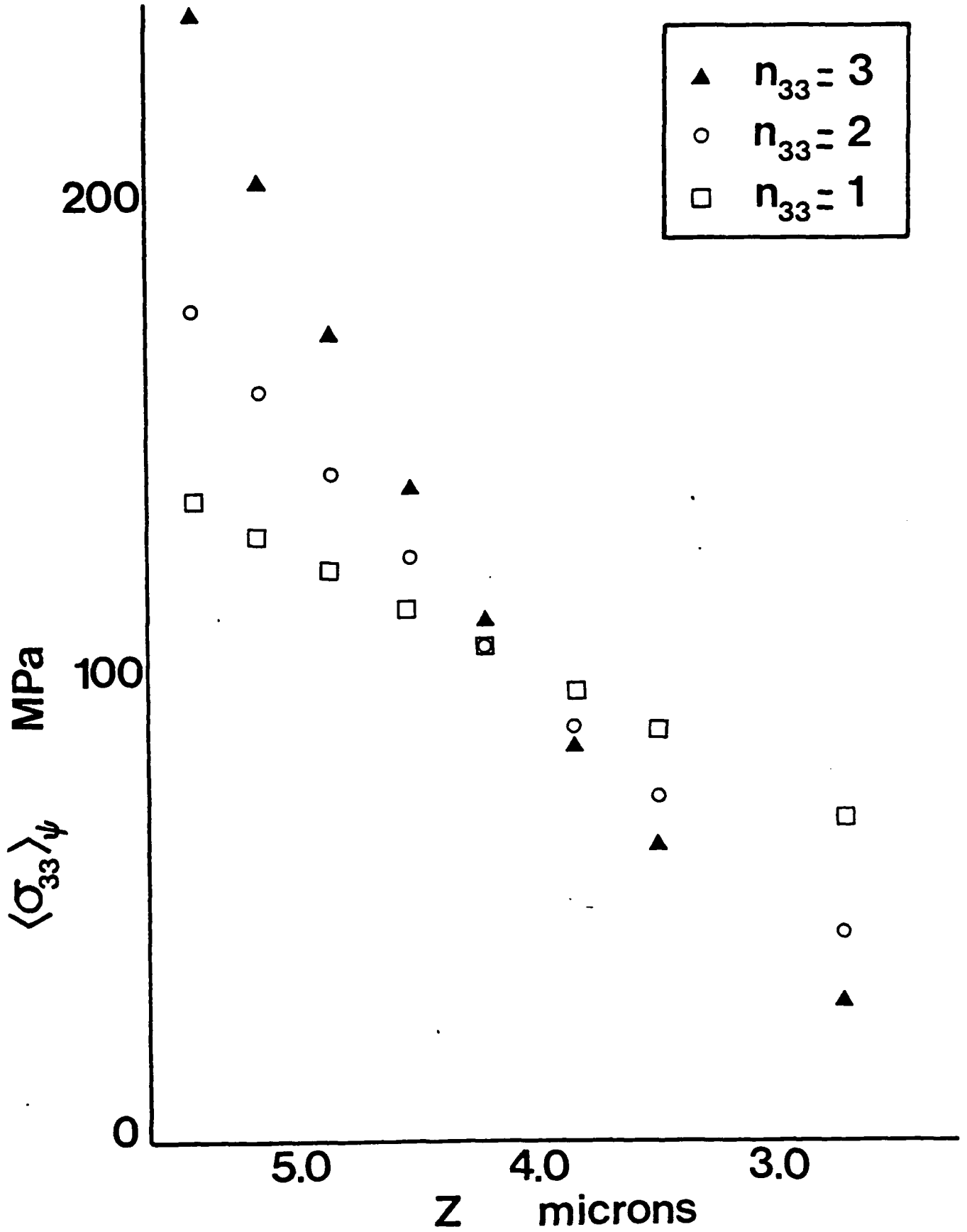

I.C. Noyan

FIGURE 3a

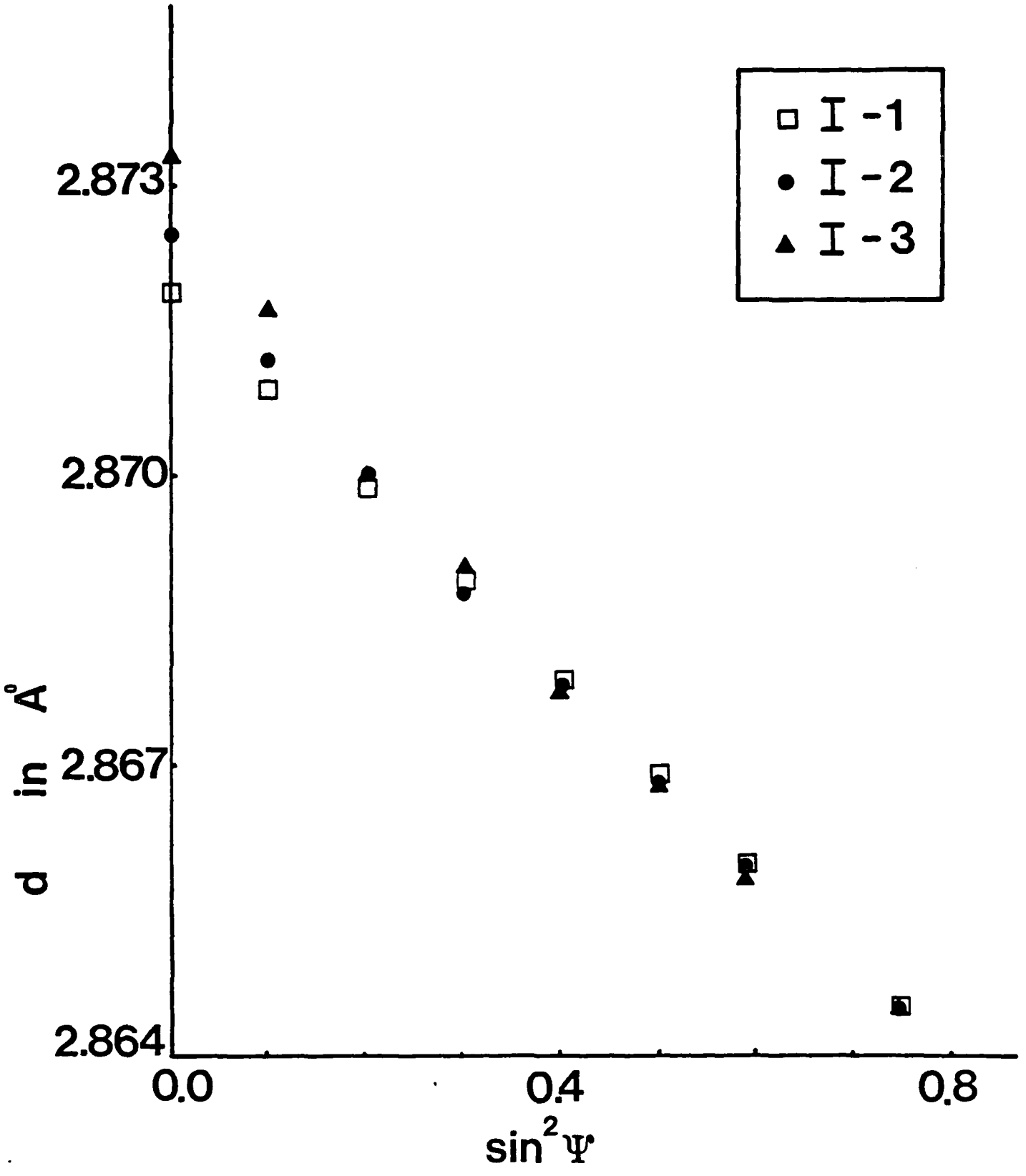

FIGURE 3b

I. C. Noyan

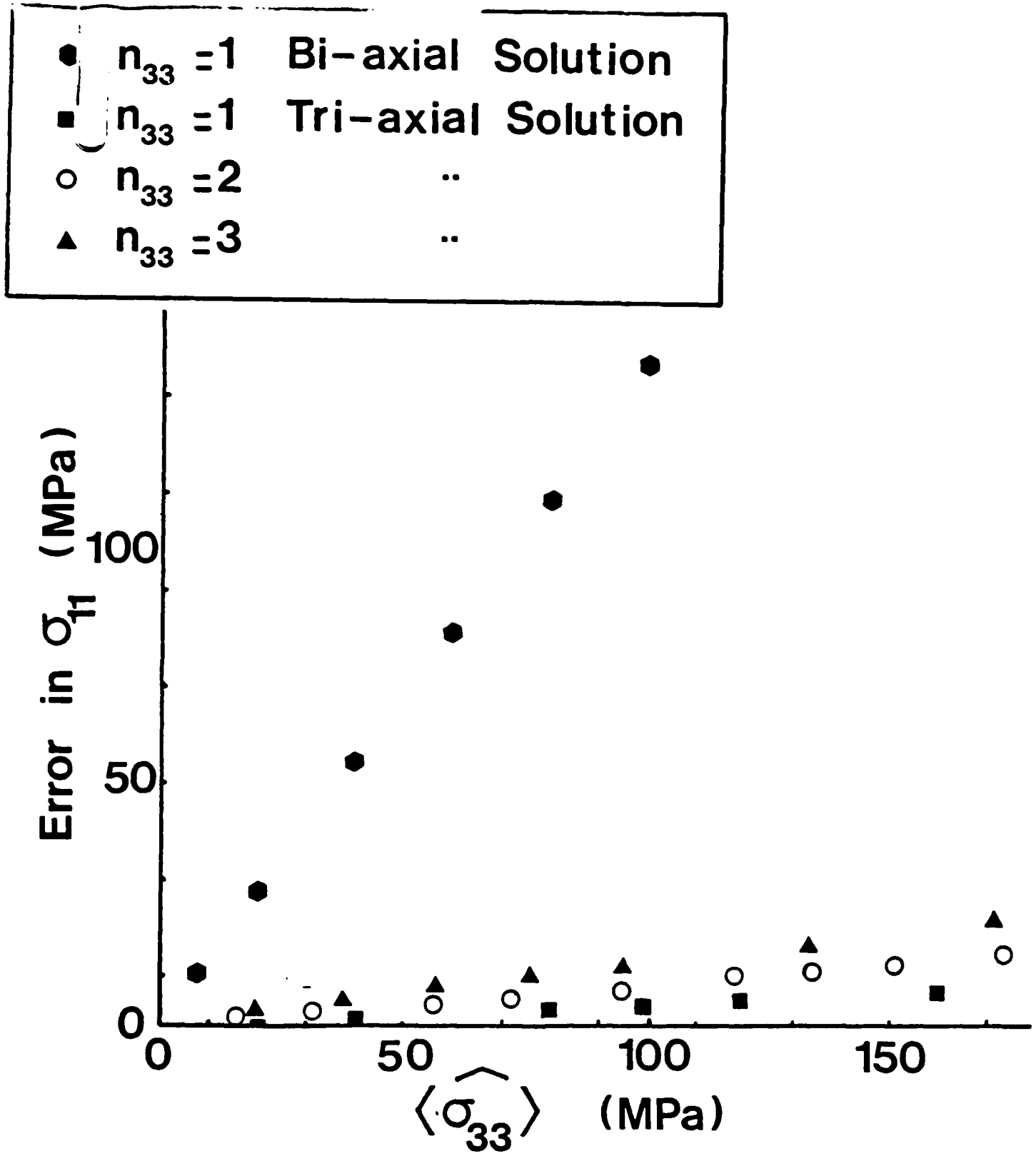

FIGURE 4

I. C. Noyan

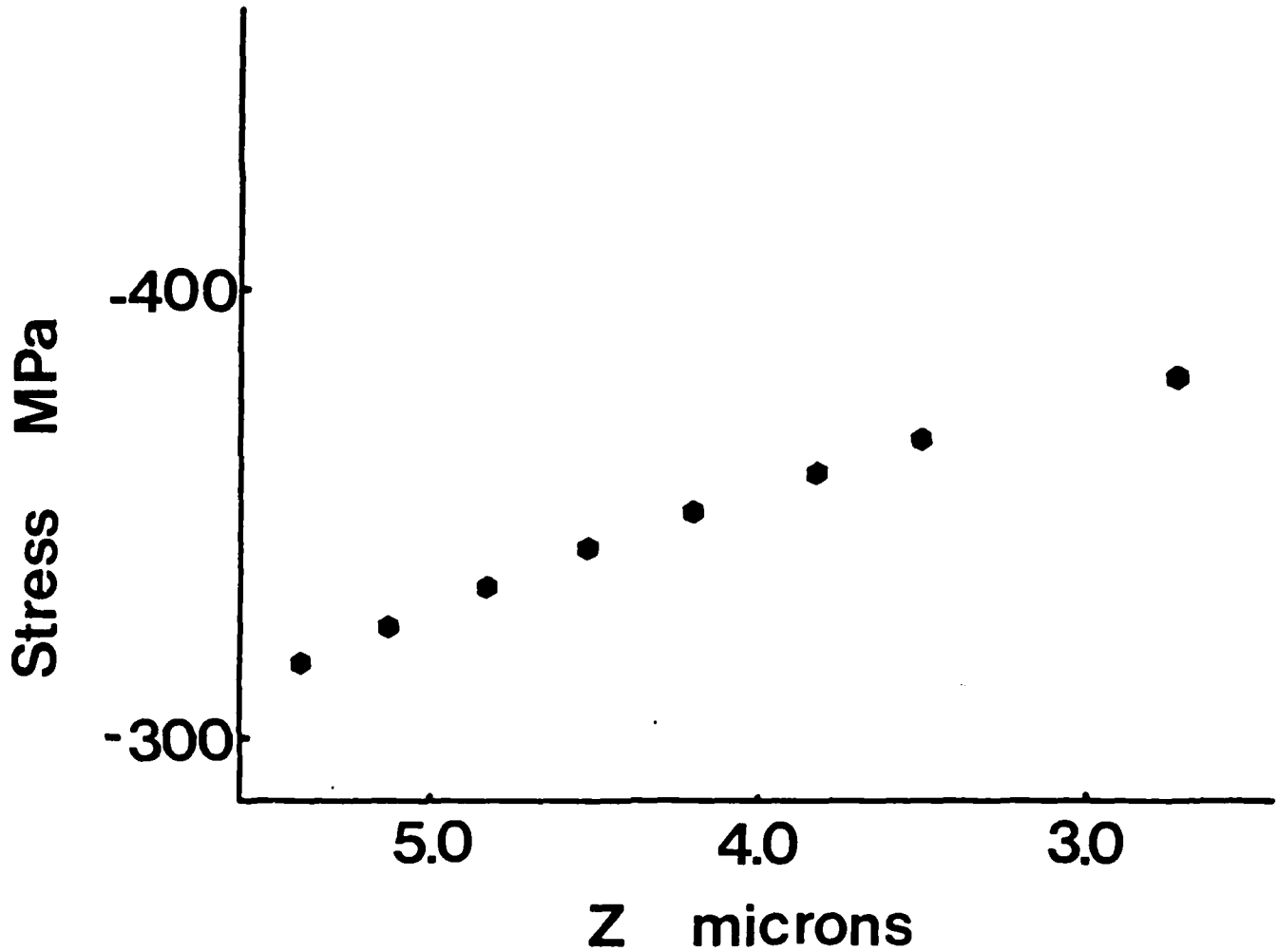

FIGURE 5a

I. C. Noyan

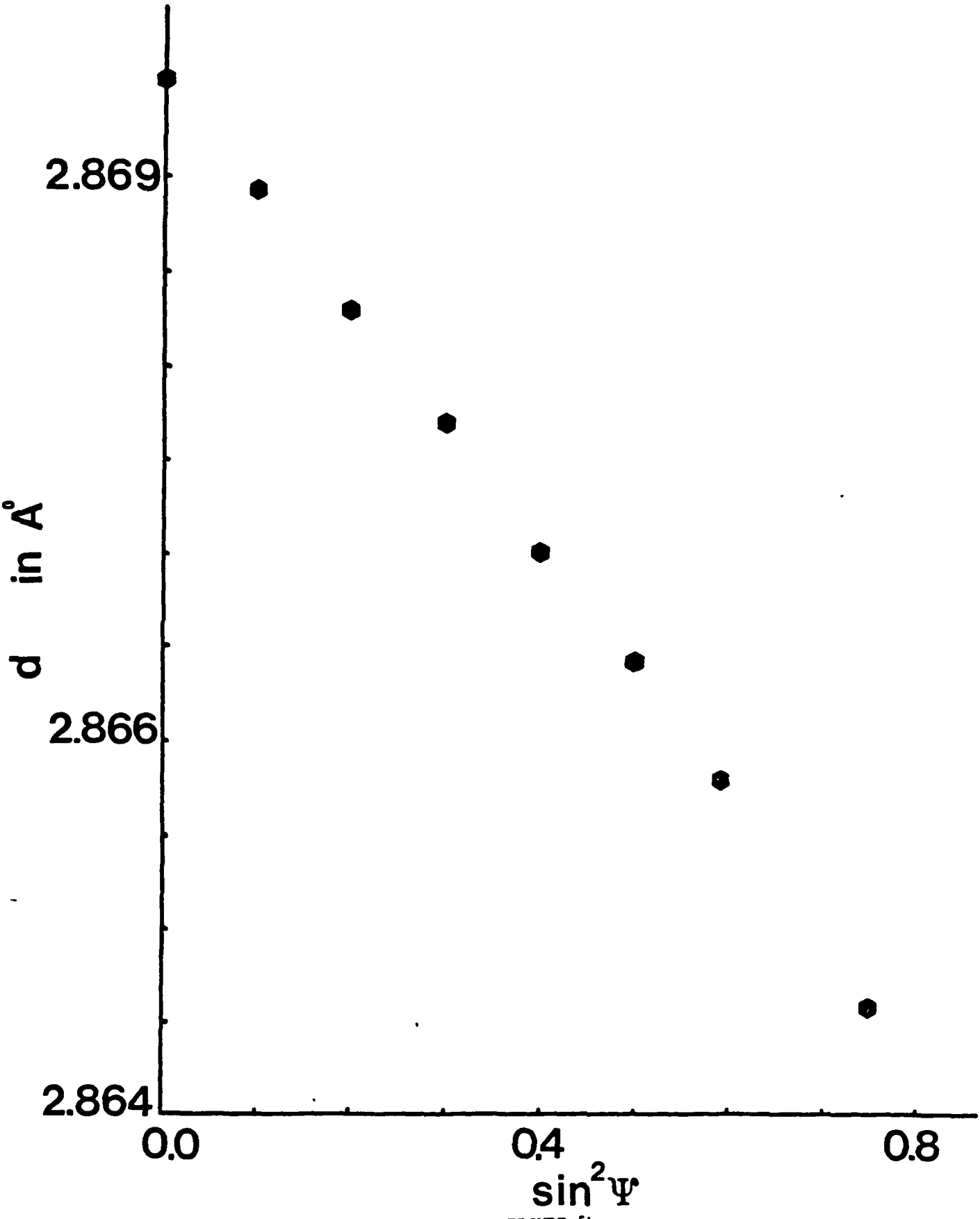

I. C. Noyan

FIGURE 5b

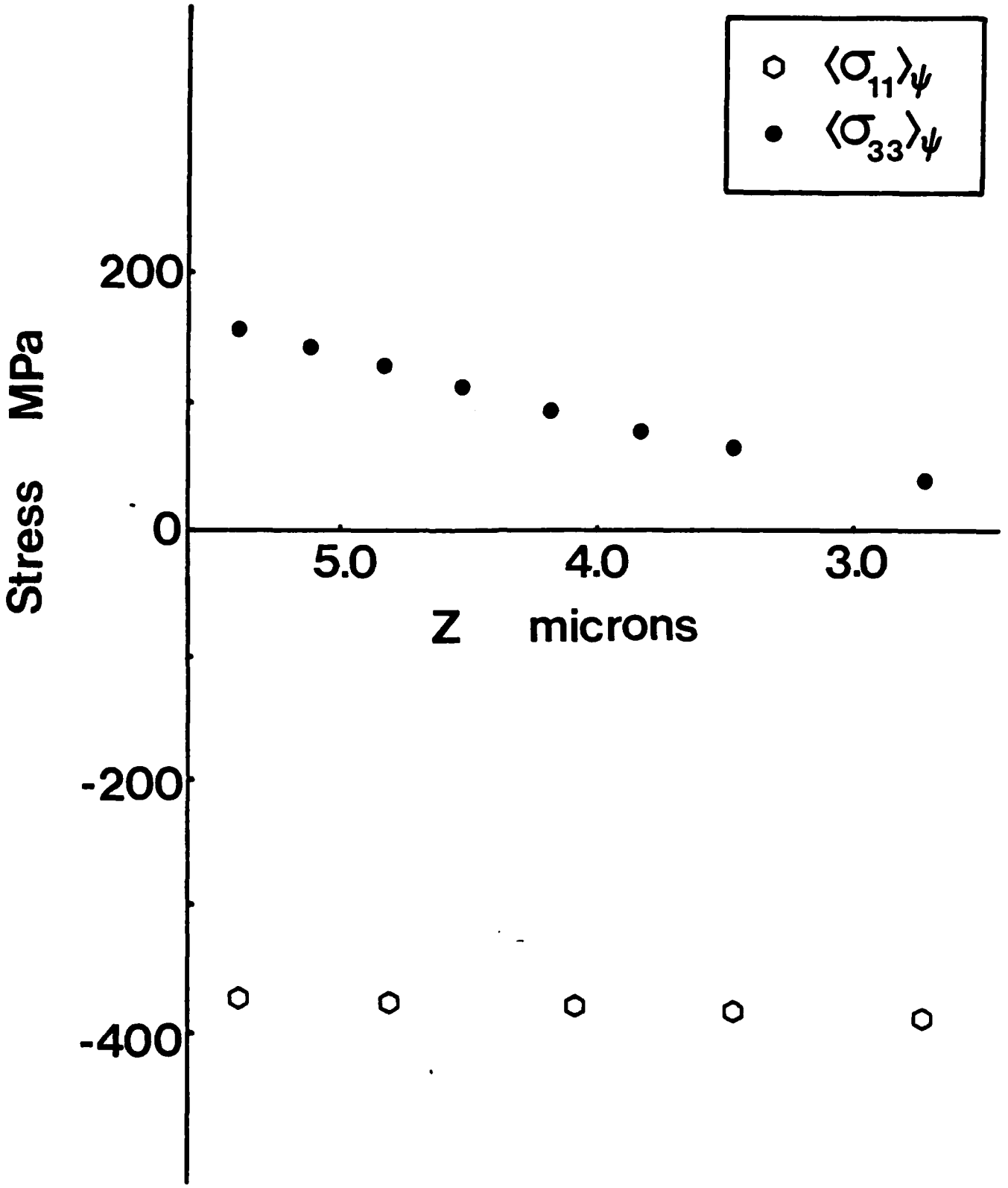

FIGURE 6a

I. C. Noyan

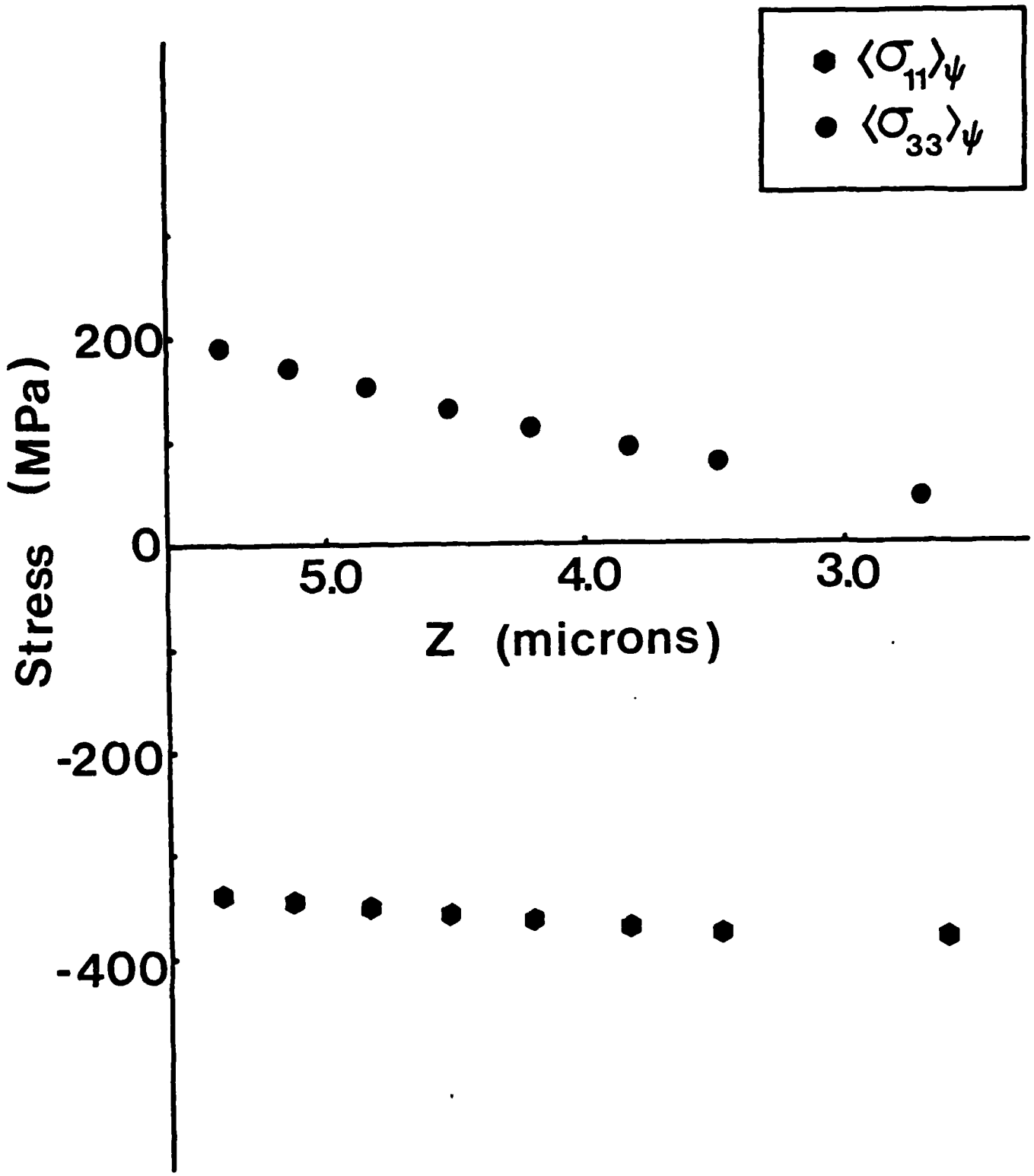

FIGURE 6b

I. C. Noyan

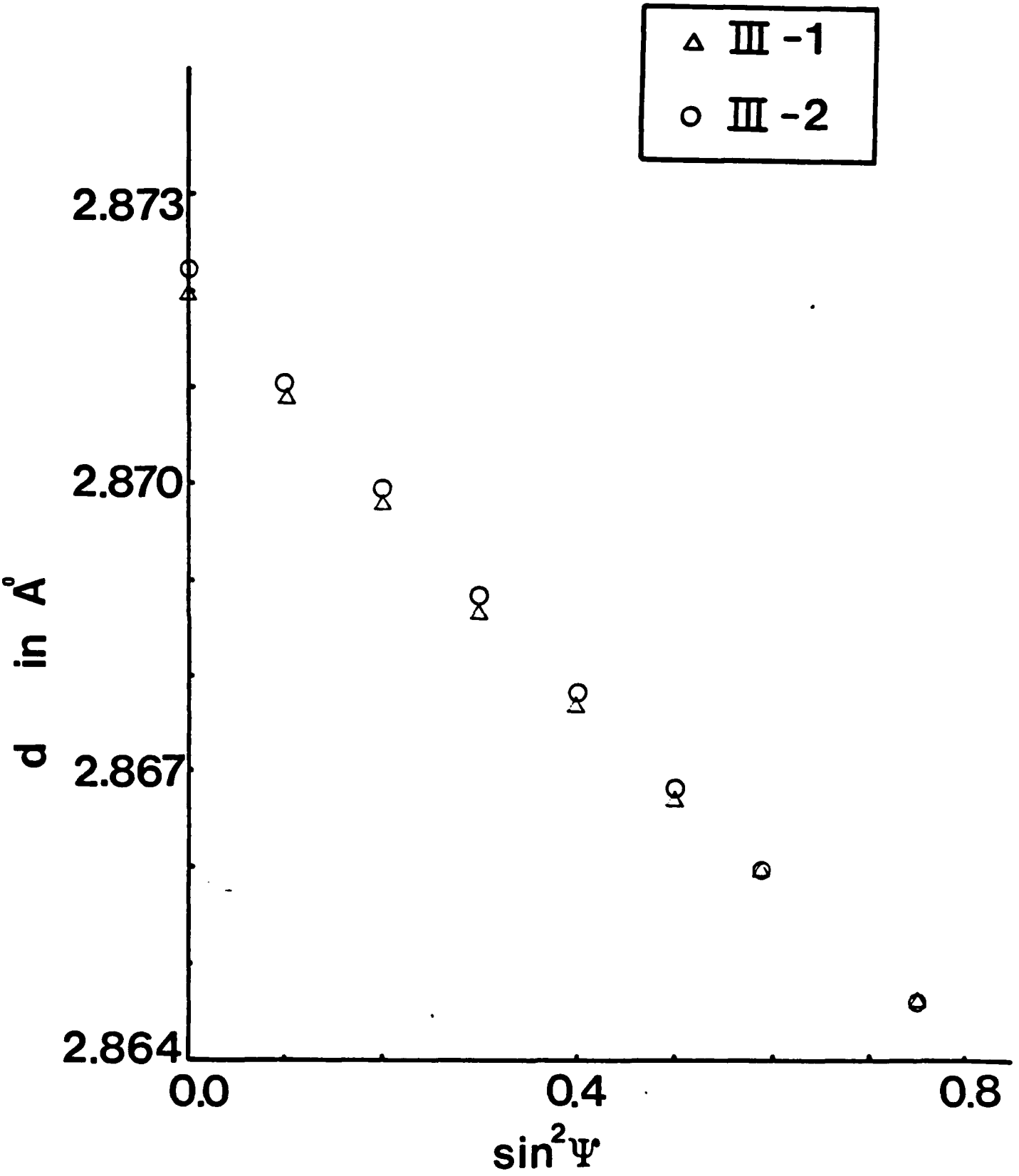

I. C. Noyan

FIGURE 6c

Security Classification

DOCUMENT CONTROL DATA - R & D

(Security classification of title, body of abstract and indexing annotation must be entered when the overall report is classified)

1. ORIGINATING ACTIVITY (Corporate author)
J. B. Cohen
Northwestern University
Evanston, Illinois 60201

2a. REPORT SECURITY CLASSIFICATION
Unclassified

2b. GROUP

3. REPORT TITLE

EFFECT OF GRADIENTS IN MULTI-AXIAL STRESS STATES ON RESIDUAL STRESS MEASUREMENTS WITH X-RAYS

4. DESCRIPTIVE NOTES (Type of report and inclusive dates)
Technical Report No. 6

5. AUTHOR(S) (First name, middle initial, last name)

I. C. Noyan

6. REPORT DATE	7a. TOTAL NO. OF PAGES	7b. NO. OF REFS
March 30, 1982	32	9

8a. CONTRACT OR GRANT NO.	9a. ORIGINATOR'S REPORT NUMBER(S)
N00014-80-C-0116	
b. PROJECT NO. Mod. No. P00002	6
c.	9b. OTHER REPORT NO(S) (Any other numbers that may be assigned this report)
d.	

10. DISTRIBUTION STATEMENT

Distribution of this document is unlimited

11. SUPPLEMENTARY NOTES	12. SPONSORING MILITARY ACTIVITY
	Metallurgy Branch Office of Naval Research

13. ABSTRACT

The assumption, that stress components in the direction of the surface normal are negligible in traditional residual stress determination methods by x-rays, has been recently disproved. In this paper we investigate the effect of normal stresses on the accuracy of these traditional methods. It is shown that appreciable error can exist in surface stresses determined by such methods, if normal stresses are present. New procedures are proposed to minimize these errors.

DD FORM 1 NOV 68 1473 (PAGE 1)

S/N 0101-807-6801

Security Classification

14 KEY WORDS	LINK A		LINK B		LINK C	
	ROLE	WT	ROLE	WT	ROLE	WT
residual stresses; x-ray measurement of residual stresses.						


ATE
LMED
-8